

# A new concept for thermal protection of all-mullite composites in combustion chambers

U. Steinhauser, W. Braue, J. Göring, B. Kanka, H. Schneider\*

*German Aerospace Center, Materials Research Institute, D-51147 Cologne, Germany*

Accepted 8 September 1999

---

## Abstract

A new thermal protection concept for all-mullite composite shingles based on a thermally-sprayed mullite layer is described. Because of the insufficient thermal long-term stability of the Nextel™ 720 fibers in the 1273 plus regime, Nextel™ 720 fiber-based ceramic composites are protected by a flame-sprayed mullite coating in order to prevent the composite from thermal degradation in service. The protection layer is deposited on the front side of the ceramic shingle facing the hot gas stream. Front and back sides of the shingles are cooled through film and convection cooling, respectively. Reducing both the composite material and the protection layer to a single phase (mullite) system is a simple, but highly efficient approach to keep thermal and elastic misfit strains at the interface at reasonably low levels. Due to the porous grain texture intrinsic to thermally-sprayed materials, thermal conductivity of the protection layer is low, yielding a considerable thermal insulation effect depending on the layer thickness and the particular heat flow scenario of the combustion chamber. The microstructure/property relationship of the thermal protection layer and its interaction with the underlying composite are discussed focussing on the constraints of real combustion chamber operation conditions. © 2000 Published by Elsevier Science Ltd. All rights reserved.

**Keywords:** Aluminosilicate fibres; Coatings; Combustion chambers; Flame spraying; Mullite coatings

---

## 1. Introduction

During recent years operating conditions in combustion chambers of jet turbines have become more and more demanding in terms of material requirements.<sup>1</sup> By increase of combustion efficiency, gas temperature was also increased inherently. Further improvement of performance is expected through the implementation of different combustion concepts like ‘rich burn-quick quench-lean burn’ (RQL) and ‘lean premixed pre-vaporized’ (LPP) which provide low NO<sub>x</sub> emissions.<sup>2</sup>

Conventional combustion liner materials, e.g. Ni-based alloys, devoid of thermal barrier coatings are limited up to a temperature of about 1120 K in a conservative approach. The discrepancy between this temperature limit and the hot gas temperature ( $\geq 2000$  K) is overcome by cooling the liner walls of the combustion chamber intensively on both sides, most commonly through film cooling techniques on the hot gas side and/

or convection or impingement cooling from the backside between the combustor liner and the casing. The air flow supply for this purpose is about 30% of the total air flow passing the combustor. If combined with an appropriate cooling technique, this figure can significantly be reduced through the implementation of ceramic matrix composites (CMC) as a liner material.<sup>3</sup> Continuous-fiber (Nextel 720) reinforced mullite composites are considered as potential candidates for ceramic shingles in combustion chambers of aircraft engines and/or stationary gas turbines.

The high gas inlet temperature required for this application is in conflict with the limited thermal stability of today’s commercial oxide-based fibers including the Nextel 720 batches. Previous research has shown that time-dependent failure (subcritical crack growth, creep) is effective for the Nextel 720 fibers at temperatures above 1000°C under thermo-mechanical loading after several service hours.<sup>4</sup> Therefore, a thermal protection concept for the fibers employed in the composites is mandatory in order to keep the effective surface temperature below this critical limit for activation of time-dependent failure thus increasing the lifetime of the component in the high-temperature regime.

---

\* Corresponding author. Tel.: +49-2203-601-2430; fax: +49-2203-68936.

E-mail address: hartmut.schneider@dlr.de (H. Schneider).

In this study, a porous, essentially matrix-free composite built of 10 stacked layers of hot-pressed Nextel 720 weaves has been evaluated as a substrate for a possible liner material. Since the thermal stability of the Nextel 720 fibers is limited to 1000°C when exposed long term to thermal and mechanical loading<sup>5</sup> a thermal protection mullite layer was applied on the substrates' surface by thermal spraying. Functionally, this flame-sprayed layer fulfills the criteria required of a typical thermal barrier layer.

## 2. Experimental

The substrate was processed by stacking up to 10 uniformly oriented disks of Nextel 720 weaves followed by hot-pressing at 20 MPa/1330°C for 15 min. In a second step these substrates were coated on one side with a flame sprayed mullite layer of variable thickness.<sup>6</sup> Fig. 1 provides a schematic view of the principle used herein. An overview of this concept with the mullite layer on top and the hot pressed Nextel 720-based CMC substrate below is displayed in Fig. 2.

Density of the two constituents was determined using the Archimedes method. Bending strength and Young's modulus were determined by conducting four-point bending tests with a computer-controlled testing machine (UTS 10) at both, room temperature as well as under high temperature conditions in air. Crosshead speed was held constant at 0.5 mm/min. The coefficient of thermal expansion up to 1350°C in air was determined using a BÄHR type 806 dilatometer. Thermal diffusivity of both materials was measured by laser flash analysis (Netsch LFA 427) in air up to 1300°C. Thermal conductivities have been calculated from experimental specific heat capacities determined via differential scanning calorimetry (Netsch DSC 404 CELL), the density and thermal diffusivity values. Hot

gas experiments were performed with impinging flame jets in a burner rig employing an acetylene/oxygen gas mixture and hardware supplied by Messer Griessheim Ltd, Frankfurt, Germany. A schematic drawing of the experimental arrangement of the burner rig relating the specimen to the impinging flame jet is given in Fig. 3. Mean velocity of the hot gas was 65 m/s and  $T_{\text{max}}$  was 2070 K.

Furthermore, the effects of annealing and subsequent testing at room temperature and true high temperature testing of annealed material have been investigated. For this purpose, plasma-sprayed mullite bulk material was annealed at different temperatures in air for 2 h and tested afterwards at room and high temperature perpendicular to the lamellar grain structure.

Microstructural investigations were conducted in a scanning electron microscope (DSM 982 Gemini) utilizing a field-emission gun.

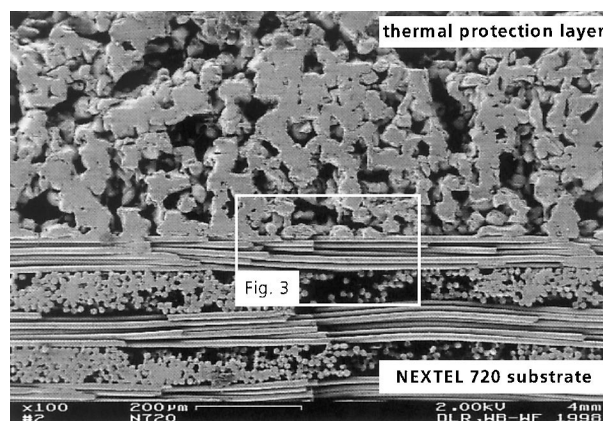


Fig. 2. SEM image of the contact area between the Nextel 720 substrate and the flame-sprayed mullite coating revealing high porosity in both constituents. The insert exhibits the interface region in more detail in Fig. 3

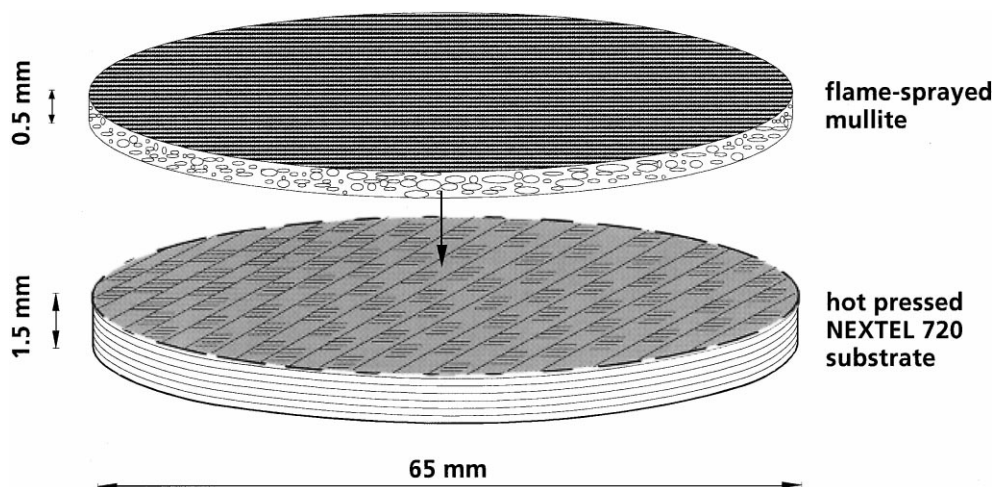


Fig. 1. Artist's conception of the all-mullite composite consisting of a flame-sprayed thermal barrier (top) and a hot-pressed CMC substrate (bottom).

### 3. Results and discussion

#### 3.1. Microstructure and properties of all-mullite composites

Despite the rather high compressive stresses applied during hot-pressing, porosity of the fiber substrate was still high ( $\approx 22\%$ ), as shown in Figs. 2 and 4. During CMC processing, the fibers sinter together at the very contact points. Open porosity was even higher in the flame-sprayed mullite layer, which was due to the inherent solidification mechanism of the flame-spraying process as shown in Fig. 2. During the passing of the acetylene/oxygen torch, the primary mullite particles (diameter 20–42  $\mu\text{m}$ ) will at least partially melt and resolidify upon impinging the substrate. Although kinetic energy of the particles is relatively small compared to true plasma spraying,<sup>7,8</sup> particle velocity during flame spraying is still high enough to penetrate the interstices in the very first layer of fibers as demonstrated in Fig. 4. The flame-sprayed mullite particles coat the top layer of the fibers exposed to the composite surface thus providing perfect mechanical interlocking

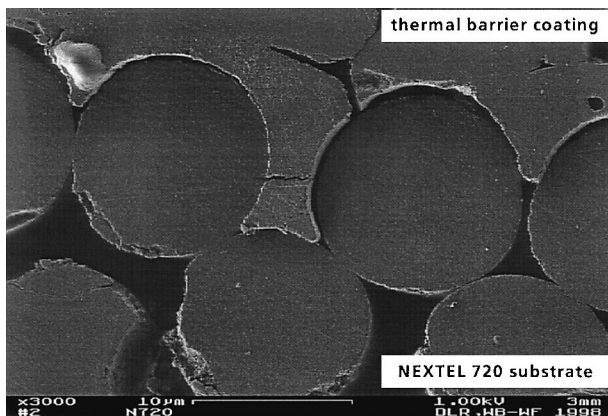


Fig. 3. Interlocking of mullite particles with Nextel 720 fibers at the interface between ceramic matrix composite substrate (bottom) and the thermally-sprayed layer (top). Cracks in the thermal protection layer have been introduced during specimen preparation.

and excellent adhesion between the fibers and the thermal protection layer.

Properties for both the all-mullite CMC substrate and the flame-sprayed mullite layer (recovered as a single-phase material in separate spraying experiments) are compiled in Table 1. Mechanical properties in terms of bending strength and Young's moduli given herein were determined at 1000°C, where a slight decrease of approximately 20% compared to room temperature values was observed. This tendency got even more pronounced when temperature was increased beyond 1000°C.

Substrate specimens annealed at 1000°C/1000 h did not show any decay in their mechanical properties compared to as pressed substrates. A more detailed overview of mechanical behavior of Nextel 720 fiber based substrates is given in Ref. 9.

The material properties relevant for combustion chamber applications are revealed in Figs. 5 and 6. Fig. 5 displays the thermal conductivities of both the substrate and mullite layer as a function of temperature. Due to the combined effects of the aforementioned high amounts of porosity and the inherently low thermal conductivity of mullite, both materials exhibit rather low values of thermal conductivity. The conductivity of the flame-sprayed mullite showed a slight tendency to increase with temperature. This is a common behavior observed for some thermally-sprayed oxide materials (e.g. plasma-sprayed alumina exhibits a thermal conductivity of 2.5 W/mK at 800°C and 5 W/mK at 1600°C<sup>10</sup>). From

Table 1  
Properties of Nextel 720 substrate and flame-sprayed layer

	Nextel 720 substrate	Flame-sprayed mullite
Open porosity (%)	22	28
Density ( $\text{g}/\text{cm}^3$ )	2.33	2.13
Bending strength (MPa)	60	20
Young's modulus (GPa)	90	20
Coefficient of emission	0.88	0.87
CTE ( $1/\text{K}$ )	$6.2 \times 10^{-6}$	$5.35 \times 10^{-6}$
Thermal conductivity (W/mK)	1	1.4

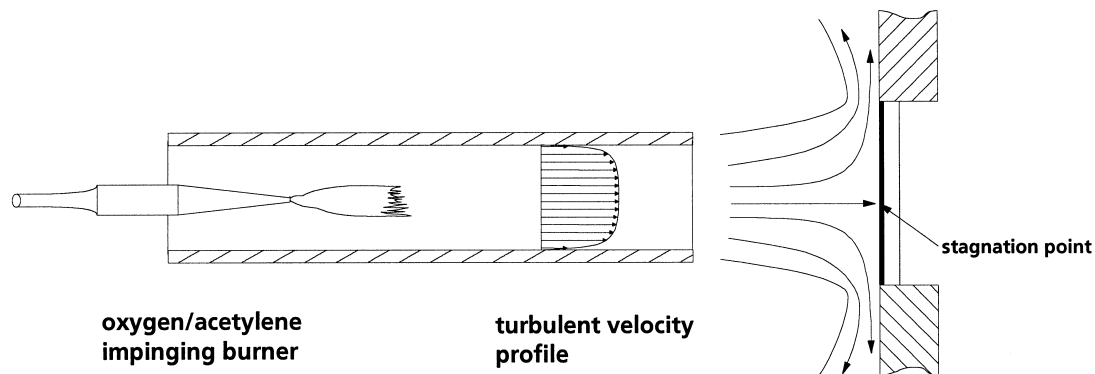


Fig. 4. Conceptual drawing of the sample arrangement during testing in an impinging flame jet. Mean velocity was 65 m/s,  $T_{\text{gas,max}}$  measured at stagnation point was 2070 K.

our own microstructural observations in the SEM and the TEM, this seems to be connected with slight sintering-induced densification at elevated temperatures due to closure of intergranular gaps and formation of sinter-necks. Obviously, the conductivity of the essentially matrix-free Nextel 720-based fiber substrate is controlled by (i) fiber-to-fiber contact areas, which increase with temperature and pressure, and (ii) the number of continuous fibers per volume with the heat being essentially transferred along the fiber axis instead of across its diameter. Thus, the thermal conductivity of the fiber substrate is low, reaching values below 1 W/mK while dense mullite ceramics exhibit values between 4.2 W/mK<sup>11</sup> and 3.9–6 W/mK<sup>12</sup> in the temperature range between 100 and 1400°C.

The coefficient of thermal expansion (CTE) of the CMC substrate as a function of temperature (Fig. 6) is in good correspondence with values from mullite plasma ceramics (MPC) given in the literature.<sup>12</sup> Due to the almost identical chemical composition of both, fiber substrate and sprayed mullite layer, CTEs exhibited similar behavior. CTE of the substrate is constantly higher than that of the layer. This is due to the occurrence of about 30% alumina phases (transition aluminas, corundum) in the fiber with alumina ( $\approx 7.8\text{--}8.1 \times 10^{-6}$

1/K)<sup>13</sup> having a higher CTE than mullite (3.9–6 W/mK). The criterion  $\text{CTE}_{\text{substrate}} > \text{CTE}_{\text{layer}}$  is beneficial because the substrate is exposed to lower temperatures than the coating and a higher CTE of the substrate would therefore help to minimize thermally induced strains at the interface (see also Section 3.3).

Samples tested in the burner showed no delamination between coating and substrate though rapid heating was established by shielding the sample before it had been exposed to the hot gas stream.

### 3.2. Long term annealing effects of mullite plasma ceramics

Materials performance after long term heat treatment is a crucial issue for a ceramic liner in a combustion chamber application.

In the as-sprayed state the material exhibits a non-brittle quasi-ductile failure behavior as shown in Fig. 7. Values for mean strength and Young's modulus are 21 MPa and 18 GPa, respectively. With increasing annealing temperature this behavior alters towards a more brittle manner, while both strength and Young's modulus rise significantly. Material annealed at 1700°C for 2 h failed spontaneously at a mean strength of 37 MPa and a mean elastic modulus of 72 GPa. This behavior is in good agreement with the results presented in previous experimental works on the effect of annealing in plasma-sprayed ceramic composites.<sup>14</sup>

Testing of annealed mullite plasma ceramics (1300°C for 2 h) under high temperature conditions revealed a decay in mean bending strength and Young's modulus (Table 2). Although creep was not considered during the tests, some preliminary experiments proved the susceptibility for creep deformation under subcritical loads. The decrease in mechanical properties at temperatures above 1100°C was probably caused by a creep deformation induced during high-temperature testing. This may be due to grain boundary sliding induced creep along thin intergranular amorphous layers at high temperature.<sup>15,16</sup>

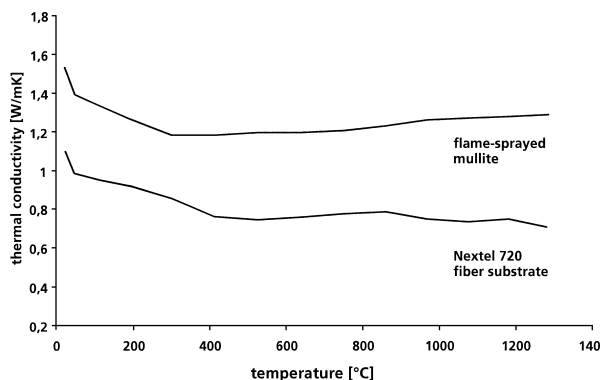


Fig. 5. Thermal conductivity of flame-sprayed mullite and Nextel 720 substrate as a function of temperature measured by laser-flash analysis.

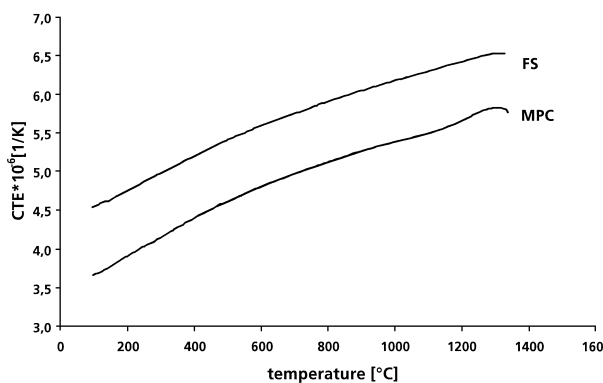


Fig. 6. Coefficients of thermal expansion for mullite plasma ceramics (MPC) and Nextel 720 fiber substrate (FS) as a function of temperature.

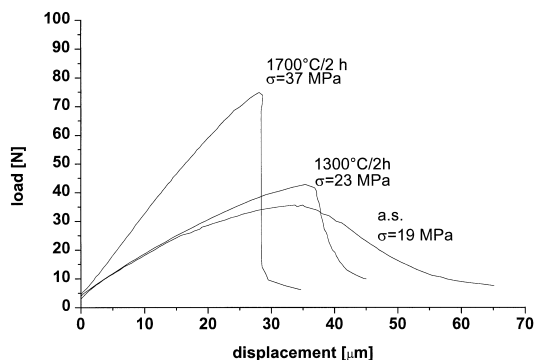


Fig. 7. Load displacement characteristics of mullite plasma ceramics in the as-sprayed (a.s.) state and after heat-treatment. Testing was performed at room temperature perpendicular to the lamellar grain alignment.

Table 2

Mean four-point-bending strength and Young's modulus for annealed MPC (1300°C/2 h)

Temperature (°C)	20	900	1100	1300
Bending strength (MPa)	20.45	23.38	20.80	17.66
Young's modulus (GPa)	29.48	29.63	17.13	9.74

### 3.3. Surface temperatures and temperature gradients in all-mullite composites in a dynamic combustion chamber scenario

Surface temperatures and temperature gradients across the liner wall are the essential parameters which control the thermal stresses generated. Therefore model calculations of surface temperatures and thermal gradients for different liner materials were performed following an one-dimensional analysis of the heat transfer process in a combustion chamber under defined boundary conditions (see also Section 3.4).<sup>17</sup> The basic operating conditions in the combustion chamber were defined as 2000 K gas temperature and 20 bar pressure ( $20 \times 10^5$  Pa), conditions that are somewhat above cruise flight conditions of today's jet engines. The total heat fluxes  $q_i$  into the combustor liner, through the liner and out of the liner are balanced according to the following equation:

$$q_{hb} + q_{rb} = q_{kL} = q_{hf} + q_{rf}$$

where subscripts h, k and r refer to convection, conduction and transfer by radiation and subscripts b, L and f designate backside, across the liner and front side of the liner wall, respectively. Expressing heat fluxes in terms of  $T_{LF}$  and  $T_{LB}$ , where  $T_{LF}$  is the liner surface temperature on the hot gas side and  $T_{LB}$  is the temperature of the backside liner wall, respectively, this equation can be solved. It should be emphasized that the only material properties needed for this model calculation are the thermal conductivity and the coefficient of emission as well as liner wall thickness as a geometric parameter.

In Fig. 8(a), the calculated surface temperatures are presented for the case of (i) a 1.5 mm thick Ni-based alloy liner material and (ii) its replacement by the Nextel 720 fiber substrate. No thermal barrier coating is involved at this stage. Gas operating conditions (pressure, temperature) and cooling air mass flow distribution remained unchanged for comparison purposes. The resulting temperature gradient is 16 K/mm in the metal compared to almost 160 K/mm in the ceramic substrate. The gradient ratio corresponds to the ratio of thermal conductivities between the metal and the Nextel<sup>TM</sup> 720 fiber substrate. Two important consequences from this scenario can be derived. First, 1305 K (1032°C) as the resulting temperature on the hot gas side is at the upper limit of thermal stability of Nextel 720 fibers and there-

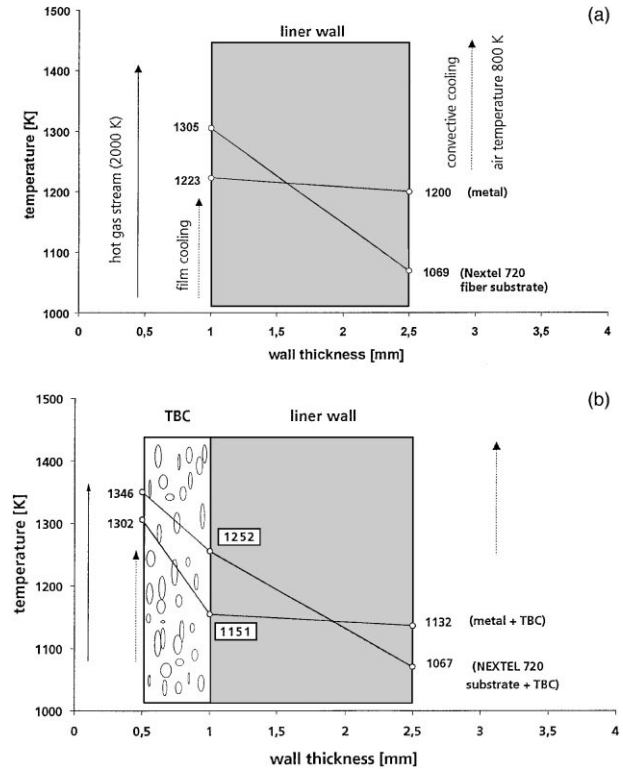


Fig. 8. Calculated surface temperatures for different wall configurations (thickness 1.5 mm) of a combustion liner following a simple one-dimensional scenario given by Ref. 17. Film-cooling (hot gas side) and convective cooling (back side) are employed. (a) The effect of replacement of a conventional metallic liner through an uncoated Nextel 720-based ceramic matrix composite (CMC) substrate. (b) The effect of an additional thermal barrier of flame-sprayed mullite (thickness 0.5 mm) on both a metallic liner and a Nextel 720 fiber-based CMC substrate.

fore an additional thermal protection layer is a mandatory requirement. The surface temperature for the metallic liner of 1223 K exceeds the thermal stability limit (1150 K) accepted for Ni-based alloys by approximately 70 K.

Second, due to the extremely low thermal conductivity of the ceramic substrate, effective backside cooling via convection is impeded. This restriction emphasizes the necessity to cool the ceramic liner mainly on the hot gas side by increasing the ratio of film cooling mass flow to total cooling mass flow. Total cooling mass flow is kept constant. It should be pointed out that the ratio of convective cooling mass flow to film cooling mass flow in this scenario was about 9. This is a reasonable figure for metallic liner materials due to their higher thermal conductivity resulting in higher efficiency through convective cooling.<sup>18</sup> For liner materials with substantially lower conductivity values this ratio will shift towards higher film cooling mass flows.<sup>19</sup> Preliminary calculations indicate that temperature decreases remarkably when film cooling mass flow is increased. Geometric boundary conditions like slot

height or operating conditions, e.g. fuel rich combustion, are the limiting factors for this approach.

If a 0.5 mm thick mullite layer is applied to both materials, surface temperatures are reduced to a tolerable level, as shown in Fig. 8(b). All the other boundary conditions (film to convective cooling mass flow, cooling air temperature and velocities) remained unchanged so that direct comparison is possible with Fig. 8(a). The temperature gradient  $dT/ds$  in the thermal barrier coating (TBC) applied on metal ( $>300$  K/mm) is much steeper compared to the Nextel 720 fiber substrates ( $<200$  K/mm). This is certainly a consequence of the higher conductivity and better heat transport through the metallic liner. The ceramic substrate represents such a high thermal resistance that the temperature at the TBC–liner wall interface is about 100 K higher than that for the metallic liner. The thickness of the mullite coating is of great importance for the heat transport across the liner. Functionally, for a higher insulating effect, a thicker layer would be desirable. Unfortunately geometric conditions like total liner thickness or the thermal stresses generated in the layer (see also Section 3.4) are limiting factors for this approach.

In the next section, the thermal gradients derived from Fig. 8(b) are employed to evaluate the thermal stresses generated in the CMC material exhibiting a thermal protection layer.

### 3.4. Analysis of thermal stresses generated across the coated all-mullite composite shingle

In Fig. 9, the thermal stresses derived from temperature gradients shown in Fig. 8(b) are plotted across the cross section of the coated Nextel 720 fiber substrate. Boundary conditions for the calculation were: a uniform temperature on both sides, unconstrained expansion (no clamping), different coefficients of thermal expansion and exclusion of time-dependent failure. By attaching both materials to each other, the condition of equal

strain in the plane of the interface has to be fulfilled. Higher temperatures in the coating combined with a lower coefficient of thermal expansion and lower temperatures in the substrate in combination with a higher CTE minimize thermally induced stresses due to thermal mismatch between the coating and the substrate. For this special case the coating is put completely under a compressive stress. If we account for time-dependent failure creep is expected to minimize these stresses in the coating.

The substrate experiences a compressive stress on the hot side and a tensile stress on the back side. Since the ‘hot part’ of the Nextel 720 fiber based composite substrate is, under a compressive stress, regarded as uncritical for the substrate, a small amount of local fiber degradation in the uppermost part of the substrate adjacent to the flame-sprayed layer can even be tolerated. It should be emphasized that this analysis is for material evaluation purposes. In a real combustion chamber, the shingle has to be fixed to the casing by bolts, clamps or other devices after processing.<sup>20,21</sup> Attachment of a shingle to the metallic casing might enclose some restrictions upon bending or expansion. This favours a smart construction, which tolerates slight movements of the attached shingle.

The essential consequence of metallic liner replacement is that higher surfaces temperatures are inherently induced in the ceramic composite because of the substrate’s inherent lower thermal conductivity. Infiltrating small gaps and pores with mullite matrix material offers only limited possibilities to increase the thermal conductivity. If we extend the actual all-mullite composite from an essentially matrix-free system as presented in this research to a composite exhibiting a significant amount of mullite matrix, 50 vol% of fibers appear to be reasonable. Considering a 20 vol% amount of residual porosity in order to preserve the favorable thermal shock resistance of the material would leave an estimated amount of 30 vol% accessible for matrix infiltration. This rather small figure cannot increase thermal

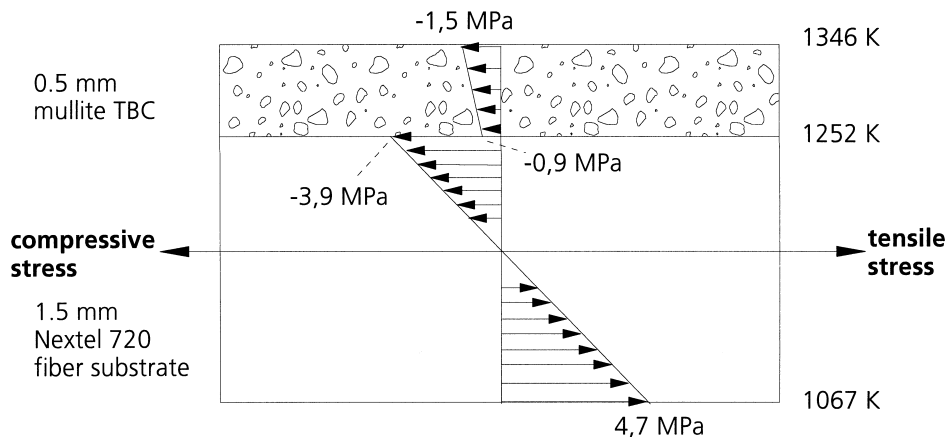


Fig. 9. Thermally induced stresses in the coated composite induced by the temperature gradient given in Fig. 8(b). No clamping or recovery from high temperature deformation have been considered.

conductivity of the material dramatically. Therefore, a thermal conductivity value of about 4 W/mK at 1000°C is a realistic estimate for an all-mullite composite. In combination with the thermal stability for the Nextel 720 fiber up to 1000°C, the benefit compared to conventional materials is rather small if cooling conditions are not adjusted to the solution employed. By adjusting the cooling techniques to the specific ceramic material's properties, there is a potential of reducing the total coolant air flow.

#### 4. Conclusions

The processing of a rather simple CMC substrate with satisfactory mechanical properties was presented. The thermally induced stresses through temperature gradients across the material are smaller than bending failure stresses. A comparatively inexpensive coating technique was employed. The flame-sprayed mullite coating exhibited good mechanical adhesion and provided a significant temperature reduction under the constraints of a real combustion chamber scenario.

The initial approach pursued in this research was to either (i) increase gas temperature in the combustion chamber or even more importantly, (ii) to decrease the air mass flow needed for cooling the liner structure. The former would cause additional consumption of cooling air to protect the liner and, further downstream, to shape a temperature profile that is not critical for the turbine blades. Considering that the temperature varies anyway depending on the combustion concept [rich burn-quick quench-lean burn (RQL) or lean premixed pre-vaporized (LPP)] applied, it appears more reasonable to keep surface temperature at the same level instead of increasing it and put more effort in reducing the required amount of cooling air. In terms of the thermally sprayed mullite layer the temperatures calculated above [see Fig. 8(a) and (b)] are regarded as not critical (melting point of mullite is about 1830°C). Even higher temperatures around 1500 to 1600°C could be tolerated on the hot gas side, when mechanical loading is moderate. This means that mullite-based CMC shingles in a combustion chamber can be exposed beyond the thermal stability of the Nextel 720 fibers through the deposition of a thermally sprayed mullite layer. Apart from the challenging task of fixing a ceramic tile to a metallic liner/casing structure, there are two further constraints to be considered: (i) effective backside cooling is difficult in a combustor application due to the low thermal conductivity, especially of the substrate, and (ii), the benefit of increased thermal stability of CMCs (1000°C) over that of Ni-based alloys (850°C) is sacrificed when only materials are replaced since a low thermal conductivity of a ceramic material results in higher surface temperatures. This almost compensates the  $\Delta T$

between metal and a CMC when the cooling scenario within the combustor does not consider the specific material properties. This implies greater importance of effective cooling techniques, e.g. through effusion or transpiration cooling, when advanced ceramic composites with low thermal conductivities are employed. Future design criteria like decreasing the total cooling air mass flow require a ceramic composite that is stable up to 1350°C for a long term application in a combustor.

#### Acknowledgements

We gratefully appreciate the stimulating discussions on aerothermodynamics in combustion chambers with H. Eickhoff and C. Hassa, DLR, Propulsion Institute, Cologne, Germany.

#### References

- Andrees, G., Schäfer, W., Smarsly, W. and Vogel, W. D., *Keramik im Flugtriebwerk*. Proceedings of the DGLR Convention (II), 1997, pp. 1287–1292.
- Tacina, R. R., Combustor technology for future aircraft. NASA Technical Memorandum 103268, AIAA-90-2400, 1990.
- Sieber, J., Das Engine 3E Technologieprogramm der MTU, DGLR-JT-96-008, DGLR-Jahrestagung 1996, Dresden.
- Wilson, D. M., Lieder, S. L. and Lueneburg, D. C., Microstructure and high temperature properties of Nextel™ 720 fibers. *Cer. Eng. Sci. Proc.* 1995, 1005–1013.
- Milz, C., Braue, W., Paul, G., Göring, J. and Schneider, H., Microstructural response of Nextel™ 720 single fiber filaments upon dynamic fatigue testing in air. *J. Eur. Ceram. Soc.*, in press.
- Braue, W., Göring, J., Kanka, B. and Steinhauser, U., Thermal protection concept for long-fiber reinforced ceramic composites. Patent pending, 1998.
- Lutz, E., Microstructure and properties of plasma-sprayed ceramics. *J. Am. Ceram. Soc.*, 1994, **77**(5), 1274–1280.
- Lutz, E., Plasmakeramik. In *Technische keramische Werkstoffe*, ed. J. Kriegesmann. Verlagsguppe Deutscher Wirtschaftsdienst, Köln, 1993, pp. 1–28.
- Göring, J., Kanka, B., Schmücker, M. and Schneider, H., Nextel™ 720-fiber fabric compacts with outstanding properties, in preparation.
- Pawlowski, L., *The science and engineering of thermal spray coatings*. John Wiley & Sons, Chichester, 1995.
- Swain, M., Structure and properties of ceramics. Materials Science and Technology, Vol. 11. VCH, Weinheim, 1994.
- Skoog, J. A. and Moore, R. E., Refractory of the past for the future: mullite and its use as a bonding phase. *Ceramic Bulletin*, 1988, **67**(7), 1180–1185.
- Schneider, H., Göring, J., Schmücker, M. and Flucht, F., Thermal stability of Nextel™ 720 alumino silicate fibers. In *Ceramic microstructure: control at the atomic level*, ed. A. P. Tomsia and A. Glaeser. Plenum Press, New York, 1998, pp. 721–731.
- LaPierre, K., Herman, H. and Tobin, A. G., The microstructure and properties of plasma-sprayed ceramic composites. *Ceram. Eng. Sci. Proc.*, 1991, **12**(7–8), 1201–1221.
- Calderon-Moreno, J. M. and Torrecillas, R., *High Temperature Creep of Polycrystalline Mullite*. Key Engineering Materials, Vols. 132–136. Trans Tech Publications, Switzerland, 1997, pp. 587–590.

16. Braue, W., Paul, G., Pleger, R., Schneider, H. and Decker, J., In-plane microstructure of plasma-sprayed Mg-Al spinel and 2/1-mullite based protective coatings: an electron microscopy study. *J. Eur. Ceram. Soc.*, 1996, **16**, 85–97.
17. Dodds, W. J. and Bahr, D. W., Combustion system design. In *Design of modern turbine combustors*, ed. A. M. Mellor. Academic Press Limited, London, 1990, pp. 431–476.
18. Juhasz, A. J. and Marek, C. J., Combustor liner film cooling in the presence of high free stream turbulence, NASA Technical Note NASA TN D-6360, Washington, DC, 1971.
19. Marek, C. J. and Juhasz, A. J., Simultaneous film and convection cooling of a plate inserted in the exhaust stream of a gas turbine combustor. NASA Technical Note NASA TN D-7156, Washington, DC, 1973.
20. Pfeiffer, A. and Wetter, H., Ceramic lining for combustion chambers. United States Patent 5 624 256, ABB Management AG, Baden, Switzerland, April 1997.
21. Craig, H. M. and Chen, O. Y., Hybrid ceramic article, United States Patent 5 553 455, United Technologies Corporation, Hartford, CT, 10 September 1996.